Coverage dependence of quantum tunneling diffusion of hydrogen and deuterium on Ni(111)

A. Wong, A. Lee, and X. D. Zhu
Department of Physics, University of California, Davis, California 95616-8677
(Received 18 August 1994; revised manuscript received 5 October 1994)

We measured the diffusion rate of deuterium on Ni(111) as a function of temperature at atomic coverage of $\theta=0.3$ and 0.05. In both cases, the crossovers from classical over-barrier hopping to under-barrier tunneling occurred at around $T=125$ K. At $T=110$ K, we measured the tunneling diffusion rates $D_{\text{tunnel}}(\theta)$ for both deuterium and hydrogen in the coverage range from $\theta=0.05$ to 0.45 and found that (1) $D_{\text{tunnel}}(\theta)$ varied by less than a factor of 3; (2) the overall features of $D_{\text{tunnel}}(\theta)$ for the two isotopes were similar; (3) $D_{\text{tunnel}}(\theta)$ weakly peaked at around $\theta=0.25$ and 0.5. Our results mostly agree with an early report by Lin and Gomer. Based on these results, we discuss the effect of the hydrogen-hydrogen interaction on hydrogen tunneling diffusion on Ni(111).

I. INTRODUCTION

Quantum aspects of adsorbate diffusion on metals have stimulated considerable research interest since the first observation of quantum tunneling diffusion of hydrogen on W(110) by Gomer and co-workers.[1] One of the intriguing observations of these authors is the unusually weak temperature dependence of the diffusion rate in the tunneling regime, a behavior which has not been observed for interstitial hydrogen and positive muons in metals. Recently, we reported an optical diffraction study of the hydrogen diffusion on Ni(100) and Ni(111).[2,3] For hydrogen and deuterium on Ni(111), our preliminary result confirmed the existence of a weakly temperature-dependent tunneling following the over-barrier hopping as reported earlier by Lin and Gomer.[4] There have been numerous theoretical attempts to explain the observations of Gomer and co-workers.[5–9] One of the concerning issues is the effect of the hydrogen-hydrogen interaction on a metal surface.[4,1,10] So far, all the experiments were performed at coverage above 5% of a monolayer or $\theta=0.05$ (corresponding to one hydrogen atom for every twenty metal atoms in the topmost layer). Depending upon the strength and range, the mutual interaction between adsorbed hydrogen atoms may significantly alter the apparent temperature dependence of the diffusion rate and thus make it more difficult to ascertain the exact microscopic tunneling mechanisms in the experiments of Gomer and co-workers and Zhu and co-workers. The nature and the parameters characterizing adsorbate-adsorbate interactions are usually not known *a priori* to sufficient accuracy and in most cases must be extracted from experimental studies of adsorbate binding-energy variations with the coverage and of structural phase diagrams and phonon spectra of the adsorbates.[11,12] Ensemble averaged rates of adsorbate diffusion by under-barrier tunneling and by over-barrier hopping are affected by these parameters. As the under-barrier tunneling of hydrogen on metals is expected to be extremely sensitive to hydrogen-hydrogen interactions, the coverage dependence of a tunneling diffusion rate is a most useful probe for studying the details of these interactions. In particular, the choices of phenomenological interaction parameters must be consistent with such a dependence.

In this paper, we report a coverage dependence study of the tunneling diffusion rates for hydrogen and deuterium on Ni(111). It is the extension of our earlier study to further investigate the finite coverage effect on the classical-quantum crossovers and on the tunneling diffusion rates $D_{\text{tunnel}}(\theta)$ below the crossover.[3] Our observation is in good agreement with an earlier report by Lin and Gomer.[4] The results enable us to examine more closely the hydrogen-hydrogen interaction on Ni(111) within a lattice-gas description.

II. EXPERIMENTAL PROCEDURES

The measurement was performed in an ultrahigh vacuum (UHV) chamber on the same Ni(111) disk which was used in our preliminary study.[3] The sample cleaning and characterization procedures have been described in our previous reports. The UHV system operates at a base pressure below 1×10^{-10} torr. It is equipped with a UTI 100C quadrupole mass spectrometer which we used for temperature-programmed-desorption measurements (TPD). In TPD measurements, we record hydrogen partial pressures and the sample temperature in real time with a computer-aided data-acquisition system. From the integrated mass yields, we deduce the relative hydrogen coverage. Christmann and co-workers studied in detail the adsorption kinetics and the overlayer structure of hydrogen on Ni(111) by carefully analyzing low electron energy diffraction, isosteric heat and thermal-desorption measurements.[11,12] They concluded that at $T\geq150$ K hydrogen dissociatively adsorb at threefold hollow sites up to one-half of a monolayer $\theta=0.5$ (one hydrogen atom for every two top-layer Ni atoms). These hydrogen atoms desorb at the highest temperature and form the β_2 peak in the thermal-desorption spectra. With significantly prolonged dosing, the hydrogen coverage increases beyond $\theta=0.5$ with the additional hydrogen going onto sites with smaller binding energies and forming the β_1 peak in thermal-desorption spectra. The exact location of these additional hydrogen atoms remains un-

0163-1829/95/51(7)/4418(8)/$06.00

resolved. We have, thus, chosen to limit our diffusion measurement to coverages below $\theta=0.5$ so that the experimental findings can be analyzed and compared to the results of other studies. We use the thermal desorption yield corresponding to the saturated β_2 peak as the absolute measure of $\theta=0.5$. This procedure yielded a relative coverage error of $\pm 10\%$.

To form hydrogen coverage gratings, we use a laser-induced thermal-desorption method with two interfering optical pulses. The details have been described elsewhere.[13] The mean coverage is determined by a calibrated ellipsometry probe which we will describe shortly. The initial coverage modulations are kept close to $\Delta\theta=0.015-0.02$ by controlling the modulation depth of the heating laser intensity pattern. The decays of the coverage gratings as monitored with the first-order diffraction of a two milliwatt He-Ne laser probe. From the decay constants and Fick's law, we extract the chemical diffusion rate.

To probe the *in situ* hydrogen coverage where the laser-induced desorption takes place, we use an optical ellipsometry method similar to the scheme used by Xiao, Xie, and Shen.[14] In this scheme, the differential reflectance of *p*-polarized and *s*-polarized lights is measured and calibrated against the coverage using thermal-desorption mass yields. The change of the differential reflectance R_p-R_s with hydrogen coverage measures the change of the dynamic dipole response in the surface region and is, in principle, similar to a work function probe.[11,12] In our ellipsometry setup as shown in Fig. 1, we use a combination of a polarized He-Ne laser and a Hinds PEM-90 photoelastic modulator to alternate the incident polarization from *s*- to *p*-polarization at 50 kHz. We use a photodiode to detect the 100 kHz component of

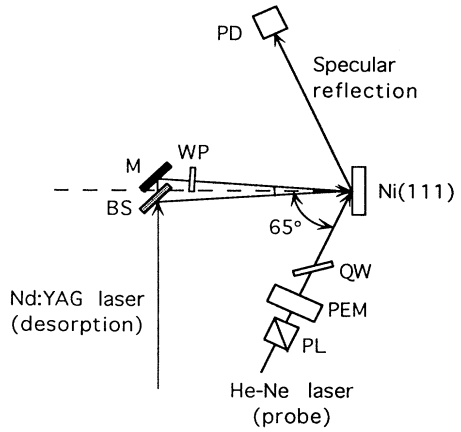

FIG. 1. Optical ellipsometry setup for monitoring the adsorbate coverage on Ni(111) and laser-induced desorption setup for creating adsorbate coverage gratings. PL: polarizer. PEM: PEM-90 photoelastic modulator (from Hinds Instrument). QW: quartz parallel window for compensating the initial reflectance difference between *s*-polarized and *p*-polarized light from a bare Ni(111) surface. BS: beam splitter. *M*: reflector. WP: wave plate for rotating the polarization of one of the interfering beams. PD: photodiode detector.

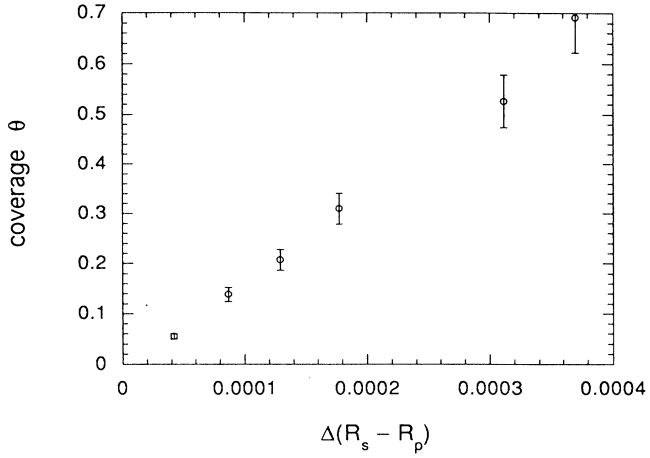

FIG. 2. Differential reflectance change $\Delta(R_s-R_p)$ from Ni(111) versus hydrogen coverage θ.

the reflected light intensity. The latter can be shown to be proportional to R_p-R_s. In Fig. 2, we display the differential reflectance R_p-R_s from Ni(111) versus the hydrogen coverage. The coverage is deduced from the thermal-desorption measurements. The measured R_p-R_s varies almost linearly with the hydrogen coverage up to $\theta=0.7$. The absolute change in R_p-R_s at $\theta=0.5$ is 2.8×10^{-4}. The linear dependence of R_p-R_s with the coverage corresponds well to the linear change of the work function in the same coverage range.[12]

In the diffusion measurement, we monitor R_p-R_s before and after the laser-induced desorption and deduce the *in situ* coverage from the calibration shown in Fig. 2.

III. RESULTS

In Fig. 3, we display the measured diffusion rates of deuterium on Ni(111) from 108 to 150 K at two coverages: $\theta=0.05$ and 0.3. The result for $\theta=0.3$ has been re-

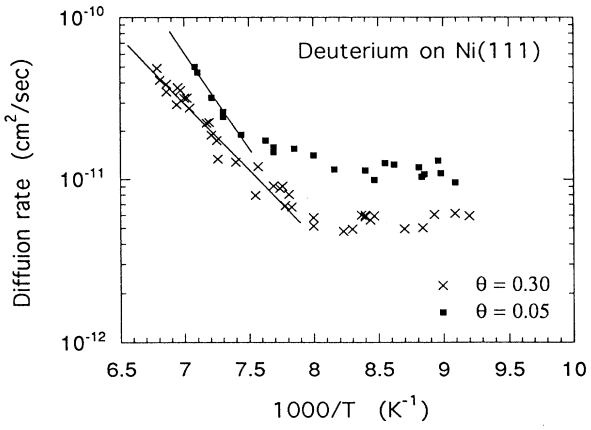

FIG. 3. Diffusion rate of deuterium on Ni(111) versus temperature. Solid squares: $\theta=0.05$. Crosses: $\theta=0.30$. The solid lines are fits to the high-temperature rates with Arrhenius functions which yield the over-barrier activation energies: $E_a=3.8\pm0.2$ kcal/mol for $\theta=0.30$, $E_a=5.2\pm0.4$ kcal/mol for $\theta=0.05$.

ported previously and is displayed here for comparison.[3] The diffusion rate at $\theta=0.05$ can be partitioned into an activated part at temperatures above 133 K and a weakly temperature-dependent part below 133 K. Following the same analysis given in Ref. 4, we attribute the first part to a classical over-barrier hopping with an activation energy $E_a=5.2\pm0.4$ kcal/mol. This energy barrier is larger than the value of 3.8 ± 0.2 kcal/mol for $\theta=0.3$. We attribute the second part to an under-barrier tunneling. The crossover occurred between $T=117$ and 133 K. This narrow transition region overlaps with the transition region for $\theta=0.3$. This indicates that the hydrogen-hydrogen interactions at $\theta=0.3$ have a weak effect on the onset of the tunneling diffusion. This aspect is consistent with the fact that at $T=108$ K the tunneling diffusion rates are only different by a factor of 2 for the two very different coverages.

At $T=110$ K which is below the transition region, we measured the tunneling diffusion rates versus the coverage for deuterium and hydrogen. The results are displayed in Figs. 4 and 5. Our results are in *qualitative* agreement with the observation by Lin and Gomer.[4] We have extended the measurement closer to $\theta=0.5$. There are three important features. The first is that the tunneling diffusion rates $D_{\text{tunnel}}(\theta)$ for both isotopes did not change by more than a factor of 3 when the coverage is varied from $\theta=0.03$ to 0.45. This indicates that the effect of the hydrogen-hydrogen interaction is weak on the tunneling diffusion rate. The second is that the diffusion rate weakly peaks at around $\theta=0.25$ and 0.5. We will argue in the next section that these peaks may be associated with the ordered overlayer structures at these two coverages and that the weakness of these peaks may be used to estimate the strength and the range of the hydrogen-hydrogen interaction on Ni(111). The third feature is that the coverage dependence of the tunneling rates for both isotopes are essentially the same up to $\theta=0.45$. It means that the distinct quantum statistics associated with the two nuclei does not have a profound effect in this coverage range. In the next section, we discuss the significance of these results.

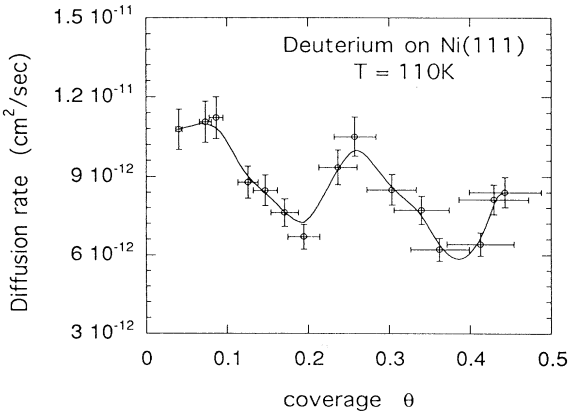

FIG. 4. Tunneling diffusion rate of deuterium on Ni(111) versus coverage θ measured at $T=110$ K.

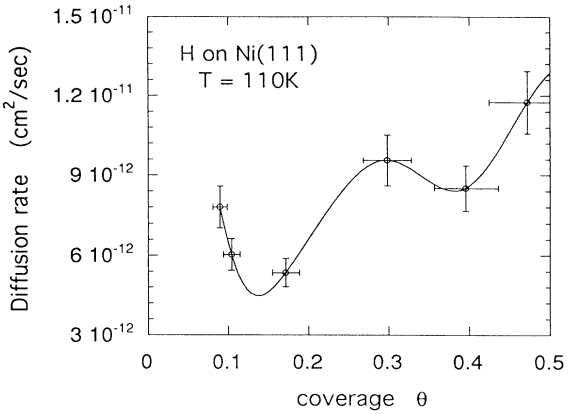

FIG. 5. Tunneling diffusion rate of hydrogen on Ni(111) versus coverage θ measured at $T=110$ K.

IV. DISCUSSION

We first discuss qualitatively the direct consequence of our experimental findings. It is helpful to review what is known of hydrogen on Ni(111) from other studies.[11,12] Hydrogen atoms occupy fcc and hcp threefold hollow sites up to $\theta=0.5$. The binding-energy difference at these two sites is suggested to be 0.02 eV by a density functional calculation.[15] Compared to the heat of desorption $E_{\text{des}}\sim1$ eV$\sim$23 kcal/mol, this difference is small and would be difficult to distinguish in a thermal-desorption measurement.[11,12] It is also small compared to the experimentally observed diffusion energy barrier of $E_{\text{diff}}\sim0.2$ eV$\sim$4 kcal/mol in the classical hopping region.[4] By comparing with the theoretical calculations by Nordlander, Holloway, and Norskov, such a barrier is consistent with a picture of hopping between a fcc site and a hcp site over a short bridge site.[16] In the absence of hydrogen-hydrogen interaction, the experimentally measured energy barrier should be an average of those from fcc sites to hcp sites and vice versa. We should remark that the binding-energy difference at the two threefold hollow sites may not be small when under-barrier tunneling is considered and it is possible that a tunneling transition occurs effectively between fcc sites or between hcp sites.[8] Christmann and co-workers found that hydrogen-hydrogen interactions on Ni(111) are primarily repulsive up to the second nearest neighbors. The fact that the maximum coverage of hydrogen on Ni(111) does not exceed $\theta=1.0$ even with a prolonged dosing ($\sim$4000 L) at 150 K indicates that the interaction between two hydrogen atoms occupying two-nearest-neighboring sites is repulsive and has the magnitude over $J_N=11$ kcal/mol. Within a lattice-gas description involving only two-body interactions, the overlayer phase diagram of hydrogen which Christman *et al.* obtained from the LEED measurement yields a second-neighbor repulsion of $J_{NN}=1.6k_BT_c=0.86$ kcal/mol.[11,12,17] From the width of the phase diagram, these authors were led to suggest that the third-neighbor interaction may be attractive.[11,17,18] Our Monte Carlo simulation shows that the magnitude of the attractive third-neighbor interaction would have to be

$J_{NNN}=-0.43$ kcal/mol, close to one-half of the second-neighbor interaction. The relation $J_{NN}=1.6k_BT_C$ includes the effect of $J_{NNN}=-0.43$ kcal/mol.[17]

In the over-barrier hopping region, our results show that the activation energy barrier varies from 3.8 ± 0.2 kcal/mol at $\theta=0.3$ to 5.2 ± 0.4 kcal/mol at $\theta=0.05$. Compared with an effective-medium theory calculation by Puska and Holloway of hydrogen binding energy on Ni(111), these values are consistent with the picture that the over-barrier hopping takes place between two threefold hollow sites by crossing a short bridge site.[16] The variation of the activation energies is the result of hydrogen-hydrogen interaction. The magnitude of the variation agrees with the findings of Lin and Gomer.[4] It also compares favorably with the energy scales of $J_{NN}=0.86$ kcal/mol and $J_{NNN}=-0.43$ kcal/mol deduced from the measurements of Christmann *et al.* We notice, however, that the trend of the activation energy variation with coverage observed is opposite to what Lin and Gomer observed. They found that the activation energy barrier at $\theta=0.3$ was larger rather than smaller. Lin and Gomer also observed a large oscillatory change in the activation energy in the coverage range between $\theta=0.2$ and 0.35. Thus at the present time, we do not believe that this discrepancy is very significant given the uncertainties in absolute coverage and in diffusion energy barriers in our measurement.

In the tunneling diffusion region, our observations are in good agreement with the report of Lin and Gomer. This is very significant since the results of Lin and Gomer were obtained with a field-emission fluctuation method. So far, this is the first case where two different measurement techniques were applied to the quantum tunneling diffusion of hydrogen on a metal and yield essentially the same results.

It is well-known that a particle density modulation decay yields a chemical diffusion rate $D(T,\theta)$, which is defined by the Fick's law. Mazenko, Banavar, and Gomer pointed out that $D(T,\theta)$ is not simply related to the tracer diffusion rate $D^*(T,\theta)$ in general.[20] It is the latter that is directly related to the microscopic diffusion mechanisms.[19,20] However if the motions of adsorbates are uncorrelated with each other, Mazenko, Gomer, and others showed that $D(T,\theta)$ is approximately related to $D^*(T,\theta)$ by a thermodynamic factor:[19–21]

$$\frac{D(T,\theta)}{D^*(T,\theta)}=\frac{\partial(\mu/k_BT)}{\partial\ln\theta}\ , \tag{1}$$

where μ is the chemical potential of the particle ensemble. Recently, Uebing and Gomer observed in their Monte Carlo simulation that Eq. (1) (known as the Darken equation) seems to be satisfied for their model interacting adsorbate systems.[20] The insensitivity of the classical-quantum crossover with respect to hydrogen coverage change and the weak variation of $D(T,\theta)$ from $\theta=0.03$ to 0.45 at $T=110$ K is quite significant. It seems to be incompatible with the large magnitude of attractive third-neighbor interaction deduced from the overlayer phase diagram and with the fact that at coverage close to $\theta=0.5$, most hydrogen atoms participate in the formation of $c(2\times2)$ structure. Consequently, it appears that either the third-neighbor interaction is much weaker than 0.43 kcal/mol and the width of the overlayer phase diagram is the result of weak but longer-range interactions or there exist a compensatory effect between the thermodynamic factor and $D^*(T,\theta)$.[4,10] The presence of longer-range interactions is consistent with the weak peak at close to $\theta=0.25$ as we will discuss next. The second possibility was first pointed out by Gomer and co-workers.[4,10] Since we cannot obtain direct experimental information on the behavior of the thermodynamic factor from the optical technique, we will discuss the second possibility later with the help of a lattice-gas model.

For both hydrogen and deuterium, the tunneling diffusion rates $D_{\text{tunnel}}(\theta)$ initially dip as the coverage increases from $\theta=0.03$ and then peak at around $\theta=0.25$. As the coverage varies from $\theta=0.25$ to 0.45, $D_{\text{tunnel}}(\theta)$ decreases again and finally weakly rises up again at close to $\theta=0.5$ The overall variation in $D_{\text{tunnel}}(\theta)$ is less than a factor of 3. It is clear that up to $\theta=0.5$, $D_{\text{tunnel}}(\theta)$ has no significant dependence on the quantum statistics of the nuclear spins. Since the majority of adsorbed hydrogen atoms on Ni(111) form the $c(2\times2)$ structure at close to $\theta=0.5$, it is reasonable to attribute the rise of the tunneling diffusion rate near $\theta=0.5$ to the approaching of such an ordering. If this is true, we should also expect some form of overlayer ordering to cause an equally weak peak at around $\theta=0.25$. As Lin and Gomer did not observe any significant change in $D_{\text{tunnel}}(\theta)$ from $T=100$ to 70 K, this peak may not be caused by having the order-disorder phase boundary accidentally at $\theta=0.25$ at $T=110$ K. One of the interesting possibilities is the formation of a $p(2\times2)$ structure where the hydrogen atoms only occupy the fcc threefold hollow sites with a primitive cell four times as large as the topmost Ni layer. This possibility was tentatively suggested by Christmann and coworkers.[11] It will require the hydrogen-hydrogen interaction to persist up to fifth or sixth-nearest neighbors as the $p(2\times2)$ structure cannot be stabilized by having the hydrogen-hydrogen interaction only up to the third-nearest neighbor. This point is also supported by our Monte Carlo simulation which will be shown shortly.

As to whether a small-polaron phonon mechanism or a nonadiabatic electron mechanism predominates the tunneling diffusion below the classical-quantum crossover, there have been numerous speculations.[5–9] It appears to us that both a modified phonon model which includes quadratic hydrogen-phonon coupling and the conduction electron model with a large hydrogen-electron coupling constant $\kappa=0.4$ are plausible candidates given that the experimental observation was over a relative narrow temperature range below the crossover.[6,8] We are currently extending the measurement from $T=108$ K down to $T=30$ K to hopefully resolve this issue.

In the second part of our discussion, we apply a lattice-gas model to further explore the implication of the experimental results and if possible, we examine the performance of the model itself in the case of hydrogen on Ni(111). We consider the interactions terms up to third-nearest neighbors whose magnitudes were determined by

fitting to the results of the low-energy electron diffraction measurement by Christmann and co-workers: $J_N=11$ kcal/mol, $J_{NN}=0.86$ kcal/mol, and $J_{NNN}=-0.43$ kcal/mol. It is reasonable that the sign of the hydrogen-hydrogen interaction alternates from positive to negative as the distance increases. This oscillatory behavior of pair interaction with distance has been observed for other adatoms on metals and the physical origin has been explored by Einstein and Schriefer within a tight-binding model calculation.[10,22] In Fig. 6, we sketch the topmost atomic layer of Ni(111) and indicate up to the sixth neighbors of a threefold hollow site. Such a lattice-gas model parametrizes the otherwise complex hydrogen-hydrogen interactions. The empirically determined parameters can then be used to calculate the thermodynamic factor $[\partial(\mu/k_BT)/\partial\ln\theta]$ and the probability distribution of the ground-state energy detuning caused by hydrogen mutual interactions. The latter is crucial for the evaluation of the ensemble average of the tracer diffusion rate $\langle D^*(T)\rangle$. The chemical diffusion rate can then be obtained from the expression $\langle D(T)\rangle=[\partial(\mu/k_BT)/\partial\ln\theta]\langle D^*(T)\rangle$ and should be compared with the rate determined experimentally.[19–21] The simulation is performed on a honeycomb lattice representing stable sites for hydrogen on Ni(111) with 1600 substrate atoms with periodic boundary conditions as shown in Fig. 6. We have assumed that fcc sites and hcp sites have the same ground-state energies in the absence of hydrogen-hydrogen interaction. A Sun SPARCstation 10 (Model 30) is used for the simulation. The thermal equilibrium in the grand canonical ensemble is obtained with 10 000 Monte Carlo steps. In each step, we fix μ/k_BT and interrogate all 3200 sites sequentially. The occupation state of an interrogated site is changed with a probability $P_{fi}\sim\exp[-(E_f-E_i\pm\mu)/k_BT]$. E_i and E_f are the energies of the lattice gas before and after the intended change. The plus (minus) sign applies when the state changes from being occupied (unoccupied) to being unoccupied (occupied). The thermal equilibrium is verified by monitoring the total energy of the lattice gas. We then perform additional 10 000 Monte Carlo steps to obtain the average coverage θ. In Fig. 7(a), we display the isotherms (chemical potential μ versus θ) thus obtained. In Fig. 7(b), we show the thermodynamic factor $[\partial(\mu/k_BT)/\partial\ln\theta]$ at $T=110$ K by numerically differentiating the isotherm shown in Fig. 7(a). One of the striking features is the large variation of the thermodynamic factor in the coverage range from $\theta=0$ to 0.45. It becomes very small over a wide region where the adsorbed atoms are in a gas-solid coexistence phase. It only increases rapidly near $\theta=0.5$. Even when the calculated curve is convoluted with a $\pm10\%$ relative coverage uncertainty, the resultant $[\partial(\mu/k_BT)/\partial\ln\theta]$ still varies by more than a factor of 10. Such a large variation has been observed experimentally by Lin and Gomer for hydrogen

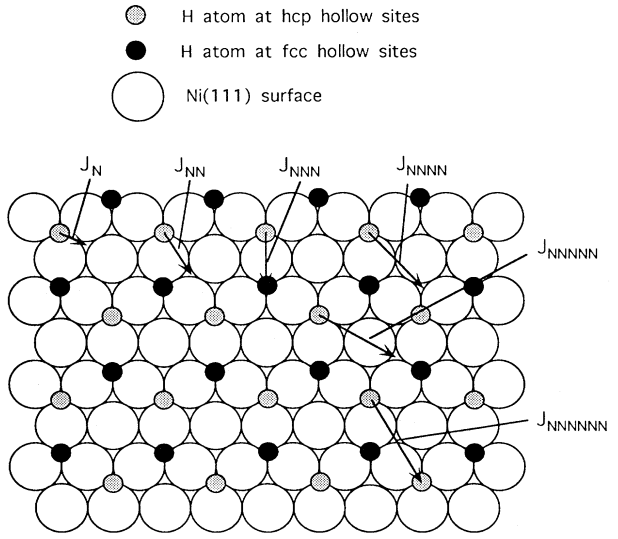

FIG. 6. Sketch of the topmost layer (large open circles) of Ni(111) surface. Solid circles: hydrogen atoms at hcp threefold hollow sites. Shaded circles: hydrogen atoms at fcc threefold hollow sites. The ensemble of either solid circles or shaded circles form a $p(2\times2)$ structure. The ensemble of solid circles and shaded circles form a $c(2\times2)$ structure. J_N, J_{NN}, J_{NNN}, J_{NNNN}, J_{NNNNN}, J_{NNNNNN} indicate up to sixth-neighbor interactions.

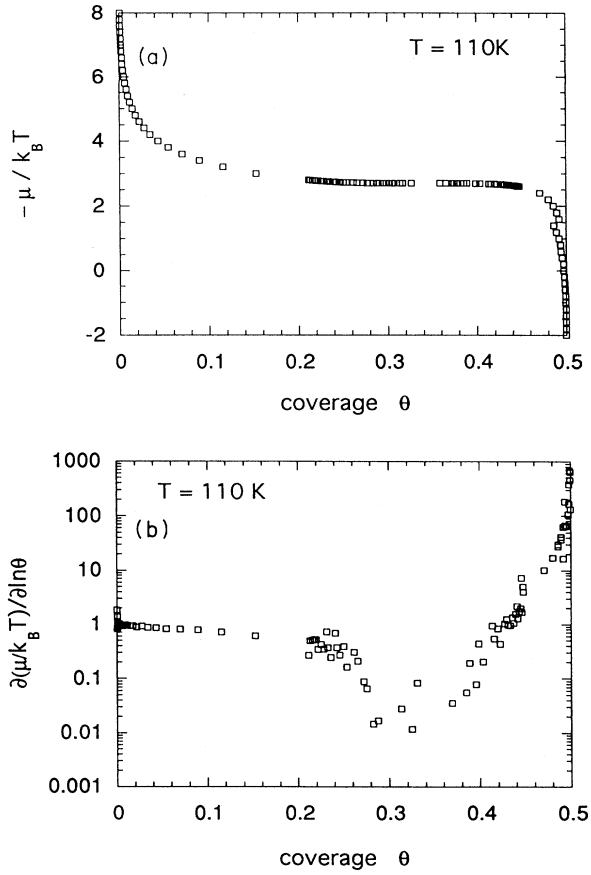

FIG. 7. (a) Calculated isotherm μ/k_BT versus θ at $T=110$ K from a lattice-gas model of hydrogen-hydrogen interactions on Ni(111) with $J_N=11$ kcal/mol, $J_{NN}=0.86$ kcal/mol, and $J_{NNN}=-0.43$ kcal/mol. (b) Thermodynamic factor $[\partial(\mu/k_BT)/\partial\ln\theta]$ at $T=110$ K calculated from the isotherm shown in (a).

on Ni(111) with a field-emission current fluctuation method. However, these authors observed that the dip in $[\partial(\mu/k_BT)/\partial \ln\theta]$ near $\theta=0.25$ did not vary with temperature while the dip of our calculated $[\partial(\mu/k_BT)/\partial \ln\theta]$ does change with temperature and is not centered at around $\theta=0.25$. This is understandable as we do not expect stable ordering to occur at $\theta=0.25$ with only up to the third-neighbor interactions. In the simulation, we also calculate the probability distribution of the energy detuning as a result of the hydrogen-hydrogen interactions. After the lattice gas reaches the thermal equilibrium, we perform 30 000 Monte Carlo steps. In each step, we interrogate each atom by allowing it to attempt a move to the three-nearest-neighbor sites if unoccupied. We count the occurrence frequency for a given differential energy or energy detuning E_f-E_i. The probability for such an energy detuning is given by dividing this frequency by the total number of adatoms and by 3, which is the number of possible moves for each atom. This probability is averaged over the 30 000 Monte Carlo steps. From this distribution, we calculate the ensemble averaged tracer diffusion rate in quantum tunneling region. We consider two cases: a nonadiabatic conduction-electron dominated tunneling and a small-polaron phonon dominated tunneling.[23–25] If we define the energy difference between the final site and the initial site due to hydrogen-hydrogen interaction as $\varepsilon \equiv E_f-E_i$, it is easily shown that the tracer diffusion rate dominated by a conduction-electron mechanism $D^*_{\rm el}(T,\varepsilon)$ is given by[23,24]

$$D^*_{\rm el}(T,\varepsilon)=D^*_{\rm el}(T,0)\left|\frac{\Gamma(\kappa+i\varepsilon/2\pi k_BT)}{\Gamma(\kappa)}\right| \times\exp\left[-\frac{\varepsilon}{2K_BT}\right], \tag{2}$$

and the one dominated by small-polaron phonon mechanism $D^*_{\rm phon}(T,\varepsilon)$ is by[25]

$$D^*_{\rm phon}(T,\varepsilon)=D^*_{\rm phon}(T,0)\exp\left[-\frac{\varepsilon}{2k_BT}-\frac{\varepsilon^2}{16E_ak_BT}\right]. \tag{3}$$

Here, κ is the hydrogen-electron coupling constant and is estimated to be 0.4 from the effective-medium theory.[8] E_a is the small-polaron activation energy arising from the hydrogen-phonon coupling.[25] In the calculation, we have taken E_a to be 0.1 kcal/mol, 0.5 kcal/mol, and 1.0 kcal/mol. We note that these rates maintain the detailed balance. In the present model, we have assumed that the tunneling matrix element remains unchanged and the effect of hydrogen mutual interaction on the tracer diffusion rate comes in only through the ground-state energy detuning ε or the multiplicative factors in Eqs. (2) and (3).[26] In Fig. 8, we show the ensemble average $\langle D^*_{\rm el}(T,\varepsilon)\rangle$ and $\langle D^*_{\rm phon}(T,\varepsilon)\rangle$. The temperature T is taken to be 110 K where the experiment was performed. Both $\langle D^*_{\rm el}(T,\varepsilon)\rangle$ and $\langle D^*_{\rm phon}(T,\varepsilon)\rangle$ decrease monotonically with the increase of coverage. From $\theta=0.025$ to 0.45, both $\langle D^*_{\rm el}(T,\varepsilon)\rangle$ and $\langle D^*_{\rm phon}(T,\varepsilon)\rangle$ drops by a factor of 100. In particular, there are no additional features either around $\theta=0.25$ or in the region where the thermodynamic factor diminishes. For $\langle D^*_{\rm phon}(T,\varepsilon)\rangle$, the result does not change significantly with the choice of E_a except for the absolute values. From the results shown in Figs. 7 and 8, we calculate the chemical diffusion rate using the expression $\langle D(T)\rangle=[\partial(\mu/k_BT)/\partial \ln\theta]\langle D^*(T)\rangle$. The result is shown in Fig. 9. Qualitatively, the model reproduces two features which are observed experimentally: the initial decrease of the diffusion rate at low coverage and the final increase of the diffusion rate as the coverage approaches $\theta=0.5$. However because there is no feature in the ensemble averaged tracer diffusion rate in the middle of the coverage range, the resultant chemical diffusion rate drops by orders of magnitude in the region where the thermodynamic factor becomes vanishingly small. This feature is not seen experimentally. In fact the experimental diffusion rate weakly peaked at around $\theta=0.25$ and

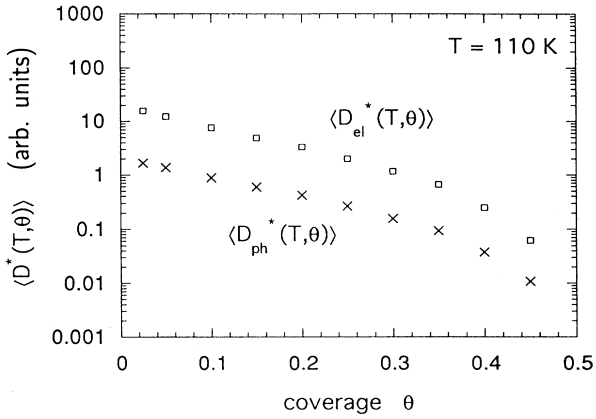

FIG. 8. Calculated ensemble average of tracer tunneling diffusion rates versus coverage θ at $T=110$ K using a lattice-gas model of hydrogen-hydrogen interactions on Ni(111) with $J_N=11$ kcal/mol, $J_{NN}=0.86$ kcal/mol, and $J_{NNN}=-0.43$ kcal/mol. $\langle D^*_{\rm el}(T,\theta)\rangle$ denote electron dominated tunneling rates. $\langle D^*_{\rm ph}(T,\theta)\rangle$ denote phonon dominated tunneling rates.

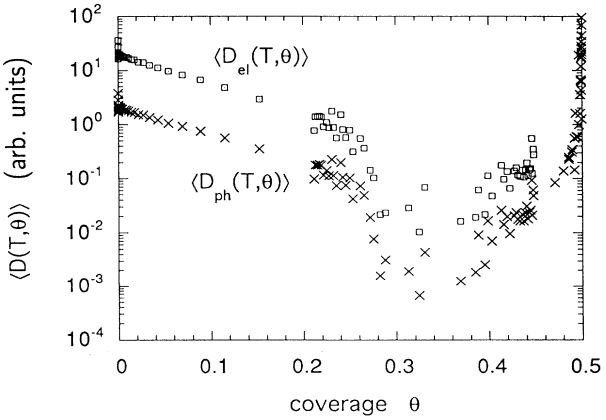

FIG. 9. Chemical tunneling diffusion rates versus θ at $T=110$ K using $\langle D(T,\theta)\rangle=[\partial(\mu/k_BT)/\partial \ln\theta]\langle D^*(T,\theta)\rangle$ and the results shown in Figs. 7 and 8.

according to the report of Lin and Gomer, the position of the peak is stable as the temperature is varied from 100 to 70 K.[4] Quantitatively, the calculated diffusion rate has a much stronger coverage dependence than what were experimentally observed for hydrogen on Ni(111), regardless whether it is dominated by the electron effect or the small-polaron phonon effect. We can draw a number of important conclusions from this result. First, the present lattice-gas model does not lead to a large compensatory feature in the tracer diffusion rate to offset the large coverage dependence of the thermodynamic factor. In fact, as the phase-transition sets in, the ensemble averaged tracer diffusion rate does not change nearly as dramatic as the thermodynamic factor does. If this result is general and model independent, it raises an interesting question as to whether there actually exist effective compensatory effects for any lattice-gas model. Second, by fitting only up to third-neighbor interaction terms to the overlayer phase diagram, this lattice-gas model is clearly inadequate to reproduce the weak and yet stable peak in $D_{\text{tunnel}}(\theta)$ at $\theta=0.25$. It will take repulsive fourth- and fifth-neighbor interactions and/or attractive sixth-neighbor interactions, if not beyond, to produce any stable feature at around $\theta=0.25$. Attempts to estimate the necessary magnitudes of these longer-distance interactions are beyond the objective of this paper. Third, the large variation and the dip in the calculated diffusion rate are the results of the large attractive third-neighbor interaction energy. Thus, any serious improvement of the lattice-gas model in order to explain the hydrogen tunneling diffusion on Ni(111) must substantially reduce the magnitude of the third-neighbor interaction while reproducing the overlayer phase diagram. It is noteworthy that the inclusion of the longer-range interactions will, in part, achieve this goal. It is unclear however whether it will yield a sufficiently weak coverage dependence to be comparable to the experimental result.

We now comment on the effect of hydrogen mutual interaction on the temperature dependence of the experimental diffusion rate, an issue which we raised in the Introduction section. Such an effect comes in through the thermodynamic factor and the ground-state energy detuning distribution.[19–21] From our earlier discussion and the fact that the experimentally observed rate varies weakly with coverage, it is reasonable to conclude that in the coverage range from $\theta=0.05$ to 0.45, adsorbed hydrogen on Ni(111) should only experience weak first-order or second-order phase transitions at above $T=110$ or 70 K. Otherwise, the chemical diffusion rate would vanish with the thermodynamic factor. Moreover, regardless of which theoretical model of the hydrogen-hydrogen interactions on Ni(111) may be appropriate, the effect of the interaction on the temperature dependence of the chemical diffusion rate should be equally weak as it is on the coverage dependence at temperatures above $T=70$ K and coverage below $\theta=0.45$. This conclusion should also be independent of whether the nonadiabatic conduction-electron effect or the small-polaron phonon effect dominates in the under-barrier tunneling region. Our Monte Carlo simulation shows that the latter may be resolved as we extend the experiment down to 30 K and at coverage no more than 2–5% of a monolayer, where the chemical diffusion rate approaches the tracer diffusion rate.

V. CONCLUSION

We have investigated the coverage dependence of the under-barrier tunneling diffusion rates of hydrogen on Ni(111) using an optical diffraction technique. Together with the field-emission fluctuation study of the same system by Lin and Gomer, we have established that the quantum tunneling diffusion of hydrogen is very weakly affected by the hydrogen-hydrogen interaction at temperatures above $T=70$ K over a wide coverage range from 5% to 45% of a monolayer. Qualitatively, the tunneling diffusion rates for both isotopes behave similarly, indicative of weak effects of quantum statistics associated with the nuclear spins. We attribute the soft peaks at around $\theta=0.5$ and 0.25 to the formations of $c(2\times2)$ and possibly $p(2\times2)$, respectively. The weak effect of hydrogen-hydrogen interaction on the coverage dependence reasonably implies an equally weak effect on the temperature dependence of the chemical diffusion rate so that the latter maybe more closely approaches the tracer diffusion rate. By applying a lattice-gas model of hydrogen-hydrogen interaction on Ni(111), we find that the inverse of the thermodynamic factor or the compressibility of adsorbed hydrogen diverges in the gas-solid coexistence region and such a divergence is not compensated for by the ensemble averaged tracer diffusion rate. The weak effect of the hydrogen mutual interactions further suggests that the third-neighbor attractive interactions should be much weaker than the estimated 0.43 kcal/mol in order to avoid strong first-order overlayer phase transition. Consequently, the width of the overlayer phase diagram of hydrogen on Ni(111) should be strongly affected by longer-range interaction such as fifth- and sixth-neighbor interactions. This point is also consistent with the observation of a soft peak at around $\theta=0.25$ Our Monte Carlo simulation raises an interesting theoretical question as to whether a more realistic model of hydrogen-hydrogen interaction on Ni(111) will yield sufficient compensatory effect to explain the weak coverage-dependent diffusion rate and large variation of the thermodynamic factor as observed by Lin and Gomer. Due to the limited temperature range where the quantum tunneling diffusion is observed, we cannot ascertain the predominant microscopic tunneling mechanisms between 70 to 110 K.

ACKNOWLEDGMENTS

The authors acknowledge the support by the Donors of the Petroleum Research Fund, administrated by the American Chemical Society, under Grant PRF No. 27240-AC5 and by the National Science Foundation under Grant No. DMR-9104109.

[1]R. DiFoggio and R. Gomer, Phys. Rev. B **25**, 3490 (1982); S. C. Wang and R. Gomer, J. Chem. Phys. **83**, 4193 (1985); C. Dharmadhikari and R. Gomer, Surf. Sci. **143**, 223 (1984); E. A. Daniels, J. C. Lin, and R. Gomer, *ibid.* **204**, 129 (1988).

[2]X. D. Zhu, A. Lee, A. Wong, and U. Linke, Phys. Rev. Lett. **68**, 1862 (1992); A. Lee, X. D. Zhu, L. Deng, and U. Linke, Phys. Rev. B **46**, 15 472 (1992).

[3]A. Lee, X. D. Zhu, A. Wong, L. Deng, and U. Linke, Phys. Rev. B **48**, 11 256 (1993).

[4]T.-S. Lin and R. Gomer, Surf. Sci. **225**, 41 (1991).

[5]A. Auerbach, K. F. Freed, and R. Gomer, J. Chem. Phys. **86**, 2356 (1987).

[6]X. D. Zhu and L. Deng, Phys. Rev. B **48**, 17 527 (1993).

[7]T. R. Mattsson *et al.,* Phys. Rev. Lett. **71**, 2615 (1993).

[8]X. D. Zhu, Phys. Rev. B **50**, 11 279 (1994).

[9]L. Y. Chen and S. C. Ying, Phys. Rev. Lett. **73**, 700 (1994).

[10]R. Gomer, Rep. Prog. Phys. **53**, 917 (1990).

[11]K. Christmann *et al.,* J. Chem. Phys. **70**, 4168 (1979).

[12]K. Christmann *et al.,* J. Chem. Phys. **60**, 4528 (1974).

[13]X. D. Zhu, Mod. Phys. Lett. B **6**, 1217 (1992), and references therein.

[14]Xu-dong Xiao, Yuanlin Xie, and Y. R. Shen, Surf. Sci. **271**, 295 (1992).

[15]S. W. Wang (private communication).

[16]P. Nordlander, S. Holloway, and J. K. Norskov, Surf. Sci. **136**, 59 (1984).

[17]In Ref. 11, the authors used a relation between the maximum transition temperature T_c and the nearest-neighbor repulsive interaction energy for a lattice gas on a square lattice to deduce J_{NN} for hydrogen on Ni(111). As shown by Domany *et al.* in the following reference this is not correct. The correct relation is $J_{NN}=2.84k_BT_c$ without the third-neighbor attraction. With the latter included, T_c increases. For $J_{NNN}=-0.5J_{NN}$ which produces the width of the over-layer $T-\theta$ phase diagram (Ref. 11), our Monte Carlo simulation yields $J_{NN}=1.6k_BT_c$.

[18]E. Domany, M. Schick, and J. S. Walker, Solid State Commun. **30**, 331 (1979); J. S. Walker and M. Schick, Phys. Rev. B **20**, 2088 (1979).

[19]G. F. Mazenko, in *Surface Mobilities on Solid Materials,* edited by V. T. Binh (Plenum, New York, 1983), p. 27 and references therein.

[20]R. Gomer, in *Surface Mobilities on Solid Materials* (Ref. 19), p. 7; C. Uebing and R. Gomer, J. Chem. Phys. **100**, 7759 (1994); G. F. Mazenko, J. R. Banavar, and R. Gomer, Surf. Sci. **107**, 457 (1981); D. A. Reed and G. Ehrlich, *ibid.* **102**, 588 (1981); **105**, 603 (1981).

[21]C. Uebing and R. Gomer, J. Chem. Phys. **95**, 7626 (1991); **95**, 7636 (1991); **95**, 7641 (1991); **95**, 7648 (1991); K. Binder and D. P. Landau, Surf. Sci. **108**, 503 (1981).

[22]T. L. Einstein and J. R. Schriefer, Phys. Rev. B **7**, 3629 (1973).

[23]J. Kondo, in *Fermi Surface Effects,* edited by J. Kondo and A. Yoshimori, Springer Series in Solid State Sciences Vol. 77 (Springer-Verlag, Heidelberg, 1988); Physica B **125**, 279 (1984).

[24]H. Grabert and U. Weiss, Phys. Rev. Lett. **54**, 1605 (1985).

[25]C. P. Flynn and A. M. Stoneham, Phys. Rev. B **1**, 3966 (1970).

[26]M. Tringides and R. Gomer, Surf. Sci. **166**, 440 (1986).